A Simplified PBM and Application to the Loss Analysis of a Dielectric Optical Waveguide

Young-Kyu Choi, Gwiy-Sang Chung, and Yong-Su Seo

Abstract

We have developed the simplified formalism of PBM in order to save calculation time and to increase the accuracy. Using this new formalism of PBM, we have evaluated the loss of the three kinds of waveguide; bent, Y-branch, and cascaded Y-branches. It takes nearly half of the cenventional PBM calculation time, even in spite of increasing of the calculation accuracy. This simplified formalism of PBM would be used efficiently in analysis of complicated three dimensional dielectric optical waveguide.

Ⅰ. Introduction

The accurate analysis of the optical integrated circuit is rather complicated because the refractive index profile is not only a function of the surface coordinates, but also a function of the waveguide depth, i. e., it is a three-dimensional problem. This complexity of analysis can be avoided by employing the effective index method reducing the three dimensional guide into an equivalent two-dimensional one and in fact, most of the existing theoretical studies were done considering a two-dimensional structure.

Various analysis methods such as Tailor's approximation technique[1, 2], the plane-wave expansion method[3, 4], the propagating beam methods(PBM) have been developed for the solution of two-dimensional waveguide discontinuities. The PBM among these is widely used in the case of the change of refractive index is very slow. This method is easily applicable to the waveguide discontinuities with arbitrary boundaries, and the field distribution of the guided wave as well as the radiated wave can be observed clearly.

Therefore, the PBM has been chosen as a general tool for simulating the properties of the dielectric waveguide and related devices. Recently, different authors reported about the PBM[5, 6, 7] where different types of approximation make the real calculation complicated.

To make the method more understandable with an easy algorithm, we developed a simple formalism of the PBM. In section 2 we shall describe the theory of this simplified method and in section 3, we compare it with the existing one. For accurate and efficient implementation of the PBM, two relevant factors, such as the applicability conditions of the PBM and the use of absorber at the two sides of the numerical window, are explained in the section 4. We show the elemination of unwanted field and programing algorithm in section 5. Using the simplified formalism of the PBM, we evaluate the losses of the three kinds of waveguide and describe the results in section 6.

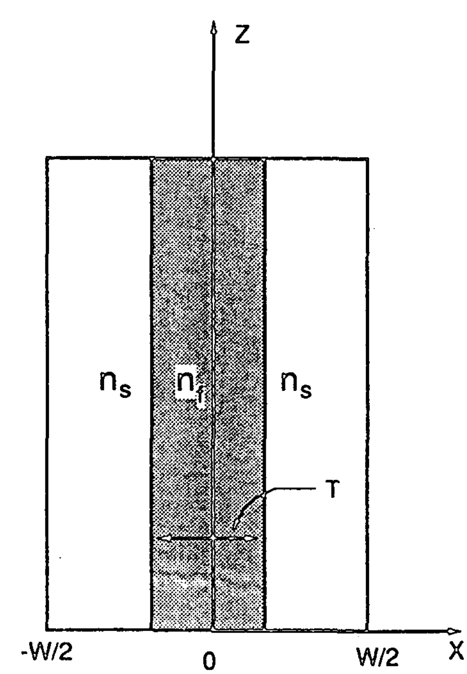

Fig. 1. Top view of a symmetric slab waveguide, W is the width of the numerical window, T is the width of the waveguide.

Manuscript received May 2, 1997; accepted September 29, 1997.
The authors are with Division of Electronics and Mechanical Engineering, Dongseo University, Pusan 617-716, Korea.

Ⅱ. Theory

Let us consider a symmetric slab waveguide of Fig. 1. Lightwaves are assumed to be propagating in z-direction. For simplicity we consider the step index distribution of the guided region. Considering uniform field in the y-direction, we rewrite the two-dimensional scalar-wave equation for TE modes as

$$\left\{\frac{\partial}{\partial x^2}+\frac{\partial}{\partial z^2}+k_o^2 n^2(x,z)\right\}E_y(x,z)=0 \quad (1)$$

where k_o is the free space wave number and $n(x,z)$ is the refractive index of the medium and $E_y(x,z)$ denotes the (x,z) dependence of the transverse electric field. One of the basic assumptions of the PBM is that the propagating of the light waves through the waveguide are considered axial i. e., almost parallel to the *z-axis*. Let us assume that the solution of the wave equation is of the form

$$E(x,z)=\exp\{-j\beta(z)z\}E(x,0) \quad (2)$$

At $z=0$, the field $E(x,0)$ represents the normal fundamental mode field distribution. Substituting Eq.(2) in Eq.(1) we get

$$\frac{\partial^2}{\partial z^2}E(x,z)=-\beta^2(z)E(x,z) \quad (3)$$

From Eq.(1) and (3) we can write "formally"

$$\beta=\{\nabla_t^2+k_o^2 n^2\}^{1/2} \quad (4)$$

where $\nabla_t\equiv\frac{\partial}{\partial x}$ and forget for a while the fact that is not a mathematical quantity but an operator. Multiplying the right side of Eq.(4) by

$$\frac{\nabla_t^2+k_o^2n^2+k_on}{\nabla_t^2+k_o^2n^2+k_on} \quad (5)$$

we get

$$\beta(z)=k_on(x,z)+\frac{\nabla_t^2}{\{\nabla_t^2+k_o^2n^2(x,z)\}^{1/2}+k_on(x,z)} \quad (6)$$

In the above equation we see that the index $n(x,z)$ is a function of both x and z coordinates. To make the analysis simple, we define

$$n(x,z)=\bar{n}+\triangle n(x,z) \quad (7)$$

where $\bar{n}$ is the average of $n(x,z)$, usually equal to the substrate index and $\triangle n(x,z)$ is the maximum $\pm$ index variation from the average value. Another essential approximation in the PBM is that the two-dimensional index variation in the second term of Eq.(6) is replaced by the average index $\bar{n}$. Using this approximation, Eq.(6) becomes a simple expression as

$$\beta(z)\equiv h(\nabla_t)+\bar{n}k_o+\triangle n(x,z)k_o \quad (8)$$

where the operator

$$h(\nabla_t)\equiv\frac{\nabla_t^2}{(\nabla_t^2+k_o^2\bar{n}^2)^{1/2}+k_o\bar{n}} \quad (9)$$

Substituting the value of β from Eq.(8) to Eq.(2) we get

$$E(x,z)=\exp[-jz\{h(\nabla_t)+\bar{n}k_o+k_o\triangle n(x,z)\}]E(x,0) \quad (10)$$

The first part of the above equation represents the total phase shift of the field at a distance z. Take the Fourier transform of the above equation with respect to x-axis and again bring it back to the real time axis by taking the inverse Fourier transform, the operator in the phase term can be easily calculated. Then Eq.(10) when $\Delta z=0$ becomes

$$E(x,z)=\exp(-jk_o\bar{n}z)\mathcal{F}^{-1}[\exp(-jH(k_{sp})z)\cdot \mathcal{F}[\exp(-jk_o\triangle n(x,z)z)E(x,0)]] \quad (11)$$

where $H(k_{sp})$ is the Fourier transform of $h(\nabla_t)$. The spatial angular frequency k_{sp} is equal to $2\pi N/W$, where N is the number of FFT sample points and W is the length of the numerical window. Substituting $\nabla_t=jk_{sp}$ in Eq.(9) we can get the value of $H(k_{sp})$. Eq.(11) is our required equation. Knowing the field at $z=0.0$, the field at a distant point z can be calculated. But here we face another complexity in calculating the index distribution $\triangle n(x,z)$ which is a function of both x and z coordinates. As we mentioned in section1 the PBM is applicable to the problem where the index of the medium changes slowly. According to this principle, we can consider that within a small distance $\triangle z$, there is no index variation. So by the represented calculation of this equation with an increasing step $\triangle z$ we can calculate the field $E(x,z)$. The above approximation makes the calculation of $\triangle n(x)$ easy, but creates a new problem in choosing the length $\triangle z$. We shall discuss this topic in the PBM applicability section 4.

Ⅲ. A Comparison with the Existing PBM

In conventional PBM[8], the counterpart of Eq.(10) is

$$E(x,z+\triangle z)=\exp[-j\triangle z\{h(\nabla_t)+k_o\bar{n}+k_o\Delta n(x,z)\}]E(x,z) \quad (12)$$

This equation reduces to our equation(10) when $z=0$. But to remove the average phase part one more approximation($\Delta n/\bar{n}\ll 0$) is used in reference[4]. By expressing $E(x,z)$ with a constant phase $\exp(-jk_o\bar{n}z)$ as

$$E(x,z)=W(x,z)\exp\{-jk_o\bar{n}z\} \quad (13)$$

Eq.(12) is rearranged as

$$W(x,z+\triangle z)=\exp[-j\triangle z\{h+k_o\triangle n(x,z)\}]W(x,z) \quad (14)$$

which is a final equation of the conventional PBM to calculate the field at a distant point z.

Comparing Eq.(14) with Eq.(10), we find that in conventional PBM one approximation is involved. This approximation degrades the accuracy and the efficiency of calculation. To make this point clear, let us get Fourier transform of the above equation and get[8]

$$W(x,z+\triangle z)=\mathcal{F}^{-1}[\exp(-j\frac{\triangle z}{2}H(k_{sp}))\cdot \mathcal{F}^{-1}[\exp(-j\frac{\triangle z}{2}H(k_{sp}))\cdot\mathcal{F}\{W(x,z)\}]]]. \quad (15)$$

From the above equation, we see that in the conventional PBM, the number of using of FFT increases twice comparing to our equation(11). Thus the calculation time is also increased. Therefore, simplified formalism of PBM can calculate the same thing in less time with better accuracy.

Ⅳ. PBM Applicability to Step Index Structures

The transverse and longitudinal resolution elements $\triangle x$ and $\triangle z$ are determined according to [9] and [10]. The first parameter to be decided is the window size, which is related to the separation distance between the two branches of a Y-junction waveguide. Let us define this distance be d_f is shown in Fig. 2. Since the evanescent modal field practically decays to zero within distance $W_{decay}=10\mu m$ from the waveguide, the maximum value of d_f is chosen to be $25\mu m$. To be in safe side we consider $d_f=W_{decay}$. In addition, the window includes two edge absorbers, each about $6\mu m$ thick which should not interfere with the guided field. Thus for waveguide of width T, a reasonable window size W seems to be

$$W=2d_f+2T+2W_{absorb}+2W_{decay}\cong 120\mu m \quad (16)$$

The number of sample points N_{FFT} is given by

$$N_{FFT}\geq\frac{2n_sW}{\lambda}\cdot\sin(\pi/8)\cong 327 \quad (17)$$

And therefore

$$\triangle x=\frac{W}{N_{FFT}}\leq 0.36\mu m. \quad (18)$$

But, according to [10]

$$\triangle x>\frac{\sqrt{2}\lambda}{2n_s}>0.203\mu m \quad (19)$$

Thus from the above two conditions a compromise seems to be

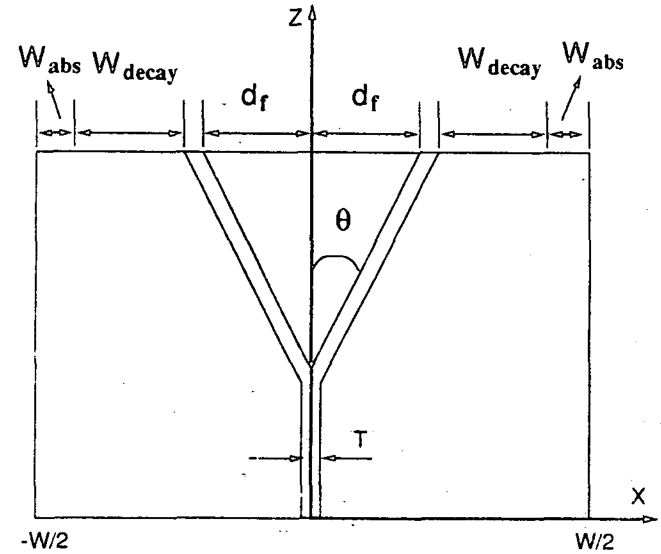

Fig. 2. A pictorial view of the numerical window. It shows the different parameters to consider in determining the width in the transverse direction.

512 sample points for the FFT and $0.25\mu m$ for $\triangle x$.

The longitudinal element $\triangle z$ is calculated according to the applicability conditions derived by Thylen[7]. We have found $\triangle z \ll 3.3\mu m$. So we have chosen $\triangle z=3\mu m$.

In determining the window size, the aspect ratio of the window should be considered. If the aspect ratio exceeds 20, then the calculated field distribution is distorted due to the addition of the reflected fields from the two boundaries. The solution of this problem is explained in the next section.

Ⅴ. Elimination of the Unwanted Field Penetration and Program Algorithm

A serious limitation of the numerical calculation of the optical waveguide devices is their length. Generally the length of such devices is at least $5mm$. For our window size, the aspect ratio is then more than 50. If we increase the window size to avoid the reflection or more clearly the penetration of the unwanted fields from the image waveguides, the calculation will be so big that even with a mainframe computer it will be difficult to calculate one time. As a solution researcher generally use imaginary absorbing materials at the two sides of the numerical window as that the field near the two boundaries becomes zero.

Instead of using such an absorbing material, we used a function named raised cosine function. The shape of this function in the numerical window is shown in Fig. 3. At the center of the window, the value of this functions equal to unity, but near the two boundaries this function decreases very slowly to become zero so that there will be no reflection from the other windows as well as from the function itself. By using this function, we

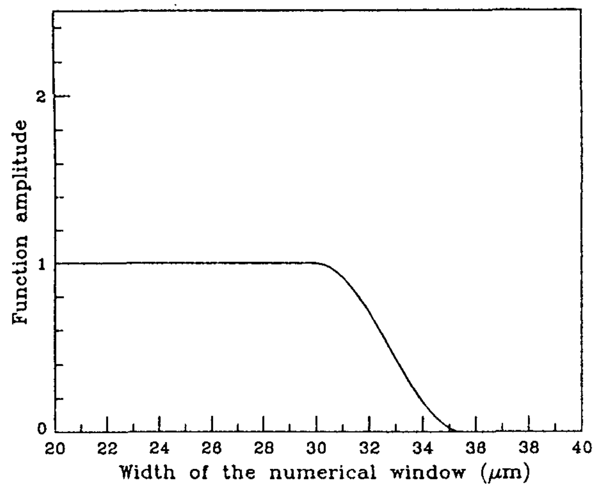

Fig. 3. The raised cosine function used in our calculation at the two sides of the boundary; in the figure only one boundary of the window is shown.

were able to calculate the field within a finite window up to a distance of about 10 *mm*.

To calculate Eq.(11), it is needed to supply the values of $E(x,0)$, k_o, $\overline{n}$, $\triangle n(x)$, $H(k_{sp})$. At $z=0$, $E(x,0)$ represents the normalized fundamental mode. For a symmetric slab waveguide the normal fundamental mode is given by

$$E(x,0)=\phi_o=C_o\cos(k_x x) \qquad \text{for}\,|x|\le\frac{T}{2}$$
$$=C_o\cos\left(k_x\frac{T}{2}\right)\cdot e^{-\gamma_s x'} \qquad \text{for}\,|x|\ge\frac{T}{2} \qquad (20)$$

where $x'=(|x|-T/2)$ and k_x and γ_s were also given in Eq.(5). The value of the constant C_o is determined by normalizing the input power to be one. The propagating constant β can be calculated using the closed-form solution.

The average index $\overline{n}$ can be considered equal to the substrate index n_s. For a fixed light source k_o is also fixed and known. The index distribution $\triangle n(x)$ is a difficult parameter to be calculated.

The procedure of calculating $H(k_{sp})$ is already stated in section 2. Now the remaining condition is that the transversal and longitudinal resolution elements $\triangle x$ and $\triangle z$ must satisfy the PBM applicability. Once all these facts are completed, the calculation can be done according to the Eq.(11)

VI. Evaluation of Waveguide Losses

1. Bending Loss

We have already developed the necessary for the simplified formalism of the PBM in the earlier sections. Using this formalism we first investigated the loss of the bending waveguide of Fig. 4.

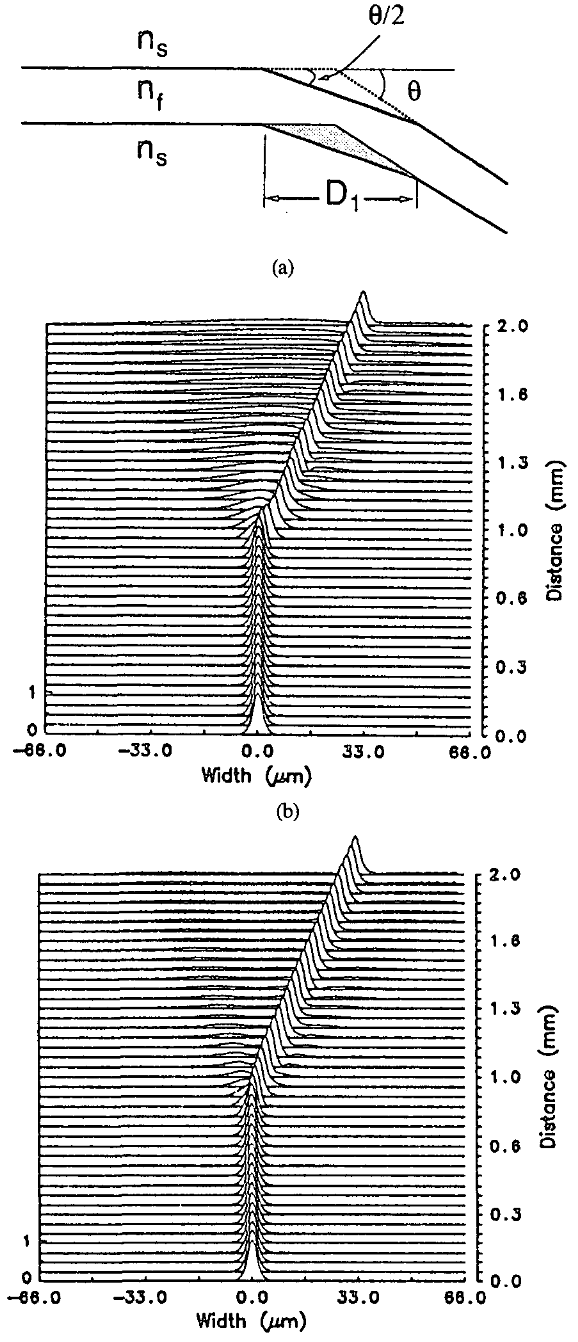

Fig. 4. (a) Refractive index modification of the bent, (b) the light field propagation in the bent without index modification, (c) with index modification.

The incident light wavelength λ is $0.633\mu m$, the width of guide T is $3\mu m$. and the normalized frequency V is chosen 3.0 so that only the fundamental mode can propagate. For step index distribution, $n_s=2.20$ and $n_s=2.303\times10^{-3}$. From the applicability of the PBM the number of sample points for 1-D FFT is found 256, the transversal and longitudinal resolution elements $\triangle x$ and $\triangle z$ are found $0.28\mu m$ and $3.0\mu m$, respectively. To avoid the unwanted field penetration, we used the raised cosine function in the calculation. The initial electric field is set as given in Eq. (20).

In calculation of the Eq.(11), we found the field propagation through the bend as shown in Fig. 4(b). With index modification the field is well confined in the guide of Fig. 4(c) than without index modification of Fig. 4(b). Without index modification we see that light propagation fluctuates as it propagates through the guide after the bend. This nature of propagation is the cause of the interference between the guided mode and the radiation mode which is generated at the abrupt bend.

The output power of the bent waveguide is calculated as

$$P_o = \left| \int_{-W/2}^{W/2} E(x,z) \cdot \phi_o^* \exp(j\beta \cdot |x| \cdot \sin\theta) dx \right|^2 \quad (21)$$

where $\exp(j\beta \cdot |x| \cdot \sin\theta)$ is the phase tilt and $\phi_o^*(x - x_{df})$ is the field distribution of the normal fundamental mode shift at x_{df} from the symmetric axis at $x=0$. By varying the bending angle we calculated the bending loss as shown in Fig. 5. The loss is decreasing with the increase of bending loss. Changing the length D_1, the loss is again observed as shown in Fig. 6 where we see that the loss is minimum when $D_1 = 186\mu m$. It is clear that by modifying the conventional abrupt bend with two steps bends which leads to the index modification, the loss is decreased considerably. We compared our results with that of [9] and found to be in good agreement.

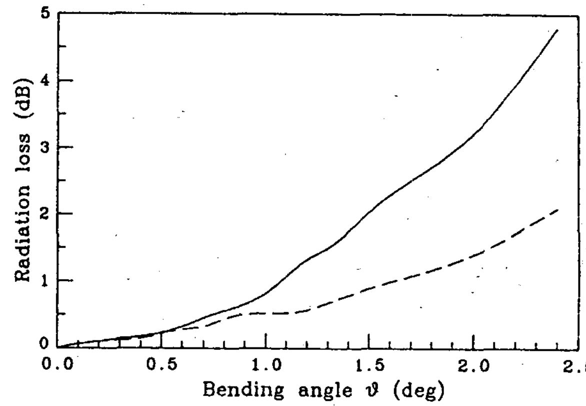

Fig. 5. Radiation loss versus bending angle of the bent.

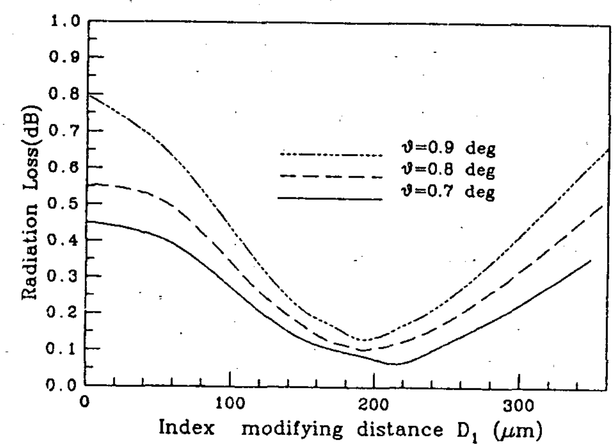

Fig. 6. Radiation loss as a function of the modifying length D1 of the bent.

2. Y-junction Loss

The modification technique of the bending waveguide is also carried out for the Y-junction as shown in Fig. 7(a). Using the same calculation procedure, we investigated the loss of the Y-junction also. The total Y branch power will then be the twice the power of a single branch. So, we first investigated Eq.(21) from 0 to $W/2$ and made this loss twice. The junction loss as a function of length D_2 is shown in Fig. 8. The minimum loss is found when $D_2 = 408\mu m$ at $\theta = 0.8\deg$. The field propagation through the guide is shown in Fig. 7. Without index modification, more light leaks out of the guide after the bend as illustrated in Fig. 7(b). But, with index modification (Fig. 7(c)), this interference is considerably reduced and the confinement of light through the guide is increased.

3. Cascaded Interferometric Waveguide Loss

Having the optimized parameters for the bending and Y-branch waveguide, let us consider the real cascaded waveguide as shown in Fig. 9. Since the first-stage is identical to the second-stage except the middle connecting waveguide, we first optimize one stage. The first part of the cascaded waveguide can be divided into four sections, L_1, L_2, L_3 and L_4(Fig. 10). Generally the loss first increases with the increase of the bending angle θ, but again decreases for higher bending angle and finally again increases at a high bending angle as shown in Fig. 11. The physical reason of this phenomena may be the interference. For small branching angle the loss is caused due to the coupling of optical power from the parallel waveguides. When they became separated quite a substantial, coupling can not occur and branching regions of the guide are so high that little light is confined in the guide. So, loss is again increases. This phenomena suggests that if we carefully choose the lengths of the wavegyide, we can confine more light at some higher branching angle.

The optimized lengths for L_2 and L_3 were found $950\mu m$ and $1200\mu m$, with $d=1.3\mu m$. The optimized parameters for the first stage waveguide is then applied to the both stages and the total loss was calculated. This time, loss was found 1.6 dB without index modification and 0.45 dB with index modification.

The field propagation through the cascaded interferometric waveguide is shown in Fig. 12. Comparing this two figures, we find that with index modification the confinement of the second-stage is same as that of the first-stage. So if we use index modification, for the multiple stages of cascaded waveguide it is

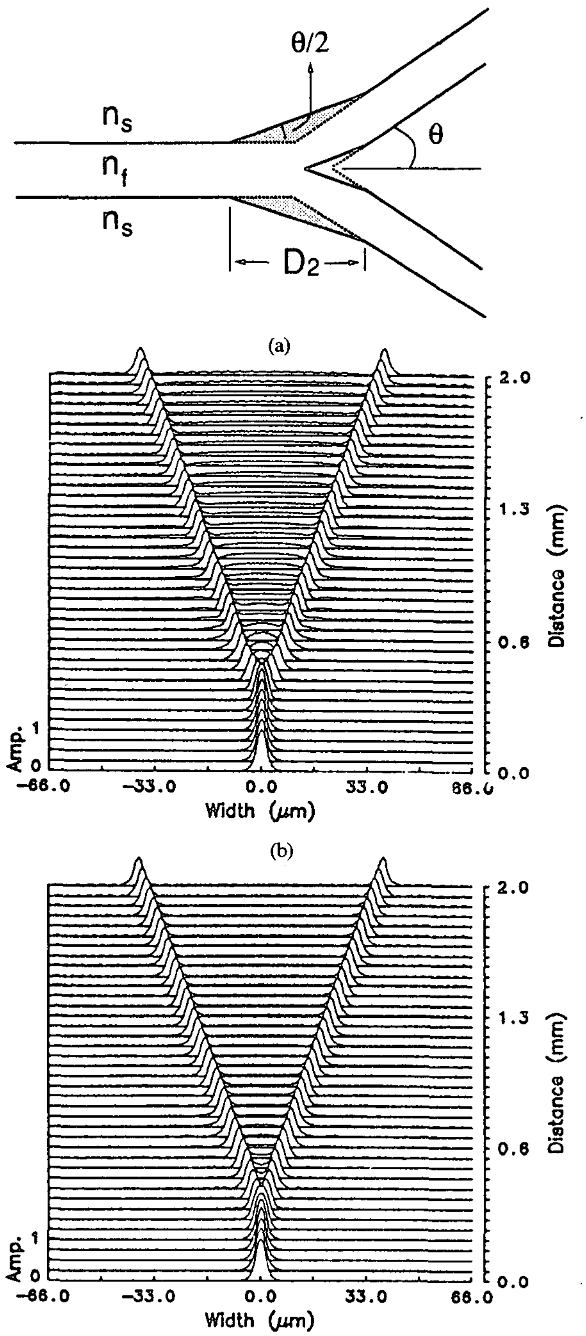

Fig. 7. Refractive index modification of the (a) Y-branch and (b) the light field propagation without index modification, (c) with index modification.

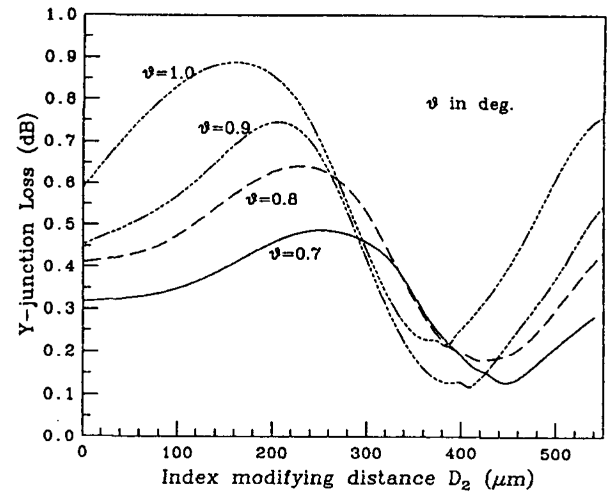

Fig. 8. Y-junction radiation loss as a function of the modifying length D_2.

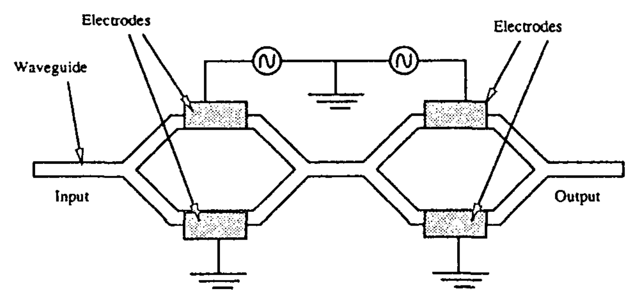

Fig. 9. Cascaded interferometric optical waveguide.

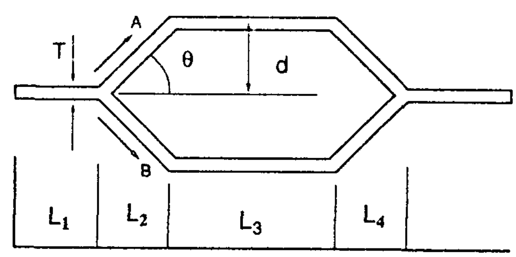

Fig. 10. First part of the waveguide.

needed only to fine the subsequent stages must be designed with separate parameters as expected earlier. One example is shown in Fig. 13. In the graph of solid curve represents the calculated loss at the output of the cascaded waveguide and the dashed curve represents the first stage loss multiplied by two. Two cases are shown separately, the total loss without modification is not twice the first stage loss, but the total loss with modification it is lower than the first stage loss expect at some extreme bending angle.

VII. Conclusions

We have presented a detailed description of the simplified propagating beam method. In a brief comparison, we clarified the advantages of our simplified method over the existing ones [9]. Comparing the Eq.(11) and Eq.(15), we know that the calculation time is saved with the half of the existing PBM in which the three times of FFT calculation are involved. Therefore, simplified formalism of PBM can calculate the same thing in less time with better accuracy. From this discussion we conclude

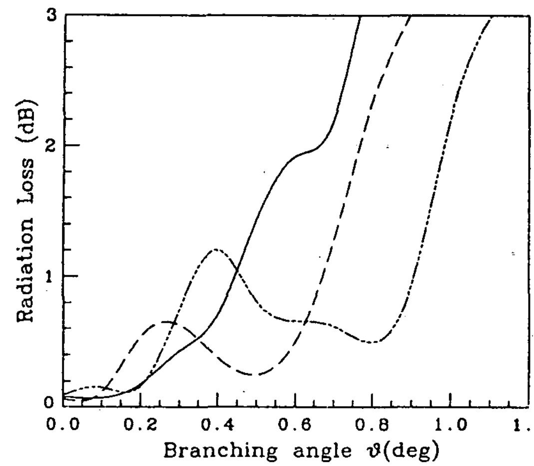

Fig. 11. Radiation loss verse branching angle for the single stage without index modification.

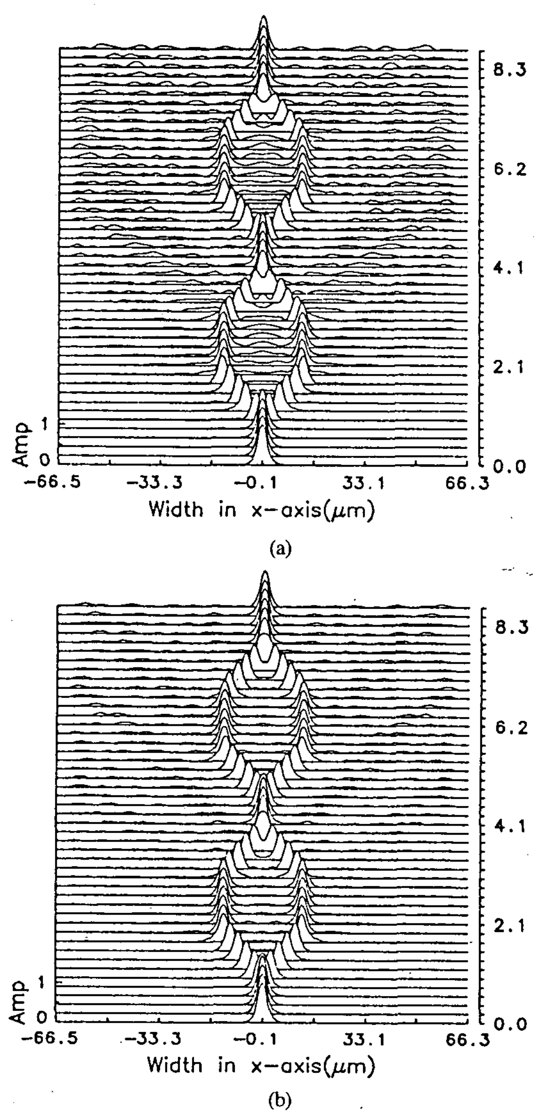

Fig. 12. The light field propagation in the cascaded wave (a) without index modification, (b) with index modification.

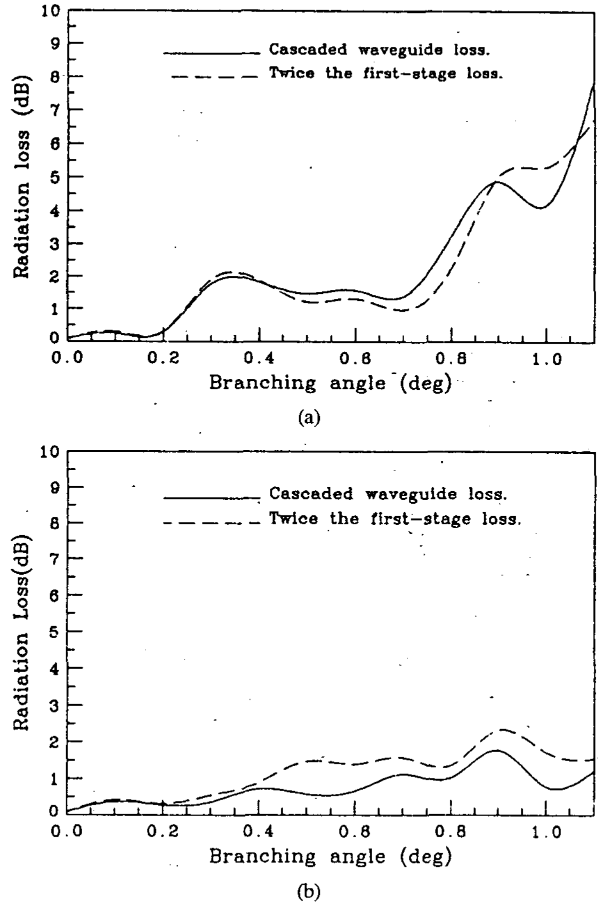

Fig. 13. The loss verse branching angle (a) without index modification (b) with index modification.

that our simplified PBM formalism may be the simplest one with better accuracy. Instead of using imaginary absorbing material at the two boundaries, we used the raised cosine function and avoided lengthy calculation. The overall accuracy depends on the applicability conditions of the PBM which must be fulfilled.

The loss due to the bending and branching waveguide was evaluated. We found that by the modification of the waveguide structure as well as the refractive index of the guide, the loss can be reduced. Using this index modification method we optimized a cascaded waveguide structure and found that the light confinement in both waveguides are same, but a conventional cascaded waveguide in which the index is not modified light confinement is different.

Acknowledgements

This work financially supported by Micro Electronics and Mechanical System Research Institute at Dongseo University.

References

[1] E. A. J. Marcatili, "Dielectric rectangular waveguide and directional coupler for integrated optics", Bell Syst. Tech. J., 48, 7, pp. 2071-2102, 1969.

[2] H. F. Taylor, "Dispersion characteristics of diffused channel waveguide," IEEE J. Quantum Electron., QE-12, 12, pp. 748-752, Jun. 1976.

[3] G. B. Hocker and W. K. Bruns, "Modes in diffused optical waveguides arbitary index profile," IEEE J. Quantum Electron., QE-11, 6, pp. 270-276, Jan. 1975.

[4] Y. Suematsu and K. Furuya, "Propagation mode and scattering loss of a two dimension a dielectric waveguide with gradual distribution of refractive index," IEEE Trans. Microwave Theory & Tech., MTT-20, 8, pp. 524-531, May 1972.

[5] M. D. Feit and J. A. Fleck, "Calculation of dispersion in graded-index multimode fibers by a propagating-beam method," Appl. Optics, Vol. 18, pp. 2843-2849, May 1979.

[6] J. Van Roy, J. Van Der Donk and P. E. Lagasse, "Beam-propagating method: analysis and assesment," Journal of Optical Society of America, Vol. 71, No. 11, pp. 803-808, Apr. 1981.

[7] L. Thylen, "The beam propagation method : an analysis of its applicability," Optical and Quantum Electronics, Vol. 15, No. 10, pp. 433-448, Sept. 1983.

[8] T. Okoshi, Planar Circuits for Microwaves and Lightwaves, Springers Series on Electrophysics 18, 1985.

[9] Z. Weissman, A. Hardy and E. Marom, "Mode-dependent radiation loss in Y-junctions and directional couplers," IEEE J. Quantum Electronics, Vol. 25, No. 6, pp. 1200-1207, Mar. 1989.

[10] T. Fujiwara, M. Izutsu, H. Murata, Y. Tanabe and T. Sueta, "Analysis of SHG in form of cerenkov radiation," IEICE Tech. Report(Japanese), Vol. 88, No. 416, pp. 77-83, Jun. 1989.

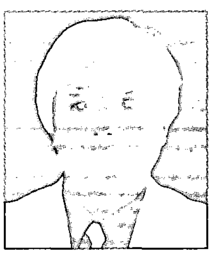

Young-Kyu Choi received the B.S. degree from Chung-Ang University, Seoul Korea in 1984 and M.S. and Ph.D. degree from Kyoto University, Kyoto, Japan, in 1989 and 1992, respectively. From 1993 to 1995, he was a lecturer of Fukui University, Fukui, Japan. Since march 1995, he has been on Faculty of Electronics and Mechanical Engineering at Dongseo University, Pusan Korea, where he is currently an associate professor. He has been engaged in research on optical modulator, optical waveguide analysis, ultra-high-speed optical detection, microwave-photonics, and optical signal processing. He is a member of IEICE and Applied Physics Society of Japan and IEEE.

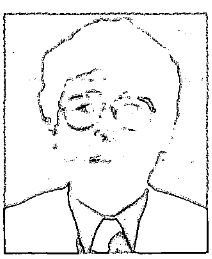

Yong-Su Seo was born in Kyungsan, Kyungpook, in 1951. He received thr B.S. degree and Ph.D. degree in electronic engineering from Kyungpook National University in 1975 and 1992. He visited Gunma Univ. in Japan for the 1990-1991 academic year. He was an Associate Professor at the Department of Electronics in Kyungnam Junior College for the 1979-1993 year. He is currently an Associate Professor at the Division of Electronic and Mechanical Engineering at Dongseo University, Pusan, Korea since 1994. His research includes the areas in image processing, multispectral image classification, remote sensing, pattern recognitions and optical signal processing.

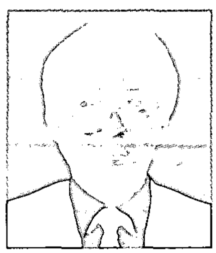

Gwiy-Sang Chung was born in Kyongnam, Korea on June 20, 1961. He received B.S. and M.S. degrees in electronic engineering from Yeungnam University in 1983 and 1985, respectively, and Ph.D. degree from Toyohashi University of Technology, Toyohashi, Japan, in 1992. He joined the Electronics and Telecommunications Research Institute (ETRI), Taejon, Korea, in 1992, where he worked on silicon-on-insulator material, MOS devices and microsensors. He is now an associate professor in the Division of Electronic and Mechanical Engineering, and a director of Micro Electronics and Mechanical System Research Institute, Dongseo University, Pusan, Korea. His research interests include silicon-on-insulator material, microsensors, microactuator, micromachining and molecular electronics. Professor Chung is a member of the Korea Institute of Telematics and Electronics, Korea Sensors Society, the Korea Institute of Electrical Engineering and the Institute of Electronics, Information and Communication Engineers in Japan.